3.5.4 HORIZONTAL WIND PERTURBATIONS AND THEIR RELATION TO TRANSIENT INTERNAL GRAVITY WAVES

A. Ebel

Institut fur Geophysik und Meteorolgie
Universitat Zu Koeln, Koeln 41, D-5000
Federal Republic of Germany

A. H. Manson and C. E. Meek

Physics Department
University of Saskatchewan
Saskatoon, Saskatchewan, S7N OWO Canada

ABSTRACT

Horizontal winds as measured with the Saskatoon MF radar exhibit wind fluctuations which have preferred directions toward north or south in the period range 0-60 min at heights between about 60 and 110 km. Longer period perturbations ($\sim$ 1-6 h) tend to have an additional maximum of direction frequencies in the E-W sector. The polarization effect analysed for more than 6 years shows regular changes with season.

The main features of the seasonal variations of the direction distributions can be explained by directional filtering of vertically propagating nonstationary gravity waves and appropriate changes of the wave source strength and position in the troposphere. The N-S polarization of the gravity-wave field appears to result in meridional wind reversals with height above the mesopause.

1. Introduction

A statistical study (over height and season) of wind perturbation directions, measured by the MF radar at Saskatoon (52°N, 107°W) is made. The direction (mod π) of maximum perturbation is found from σ_N, σ_E, and ρ_{NE}. The variance as a function of direction is an ellipse, and the axial ratio in conjunction with the number of wind values used defines a significance level (by comparison with randomly generated sequences), viz. the probability that the perturbations are not isotropic. The two kinds of perturbations used are those within an hour (WH) with respect to the hourly mean, and differences of consecutive hourly means (HD) occurring during a day -- the periods are approximately $\lesssim$ 1 hr, and $\sim$ 1-6 hr, respectively (data gaps within the hour cause some smearing of the period ranges).

On the assumption that these directed perturbations are a result of gravity waves (GW) propagating in the direction of maximum perturbation, an attempt is made to duplicate their measured total and seasonal characteristics with a combination of background wind filtering and (possibly) anisotropic GW direction distributions incident on the mesosphere from below.

2. DATA

Figure 1 shows the total (over height and month) histograms (number per 10° direction box) for the HD and WH perturbations with no applied confidence level (solid line) and all data falling below 80% confidence (dashed line). As expected, the theoretically more isotropic ellipses are distributed more

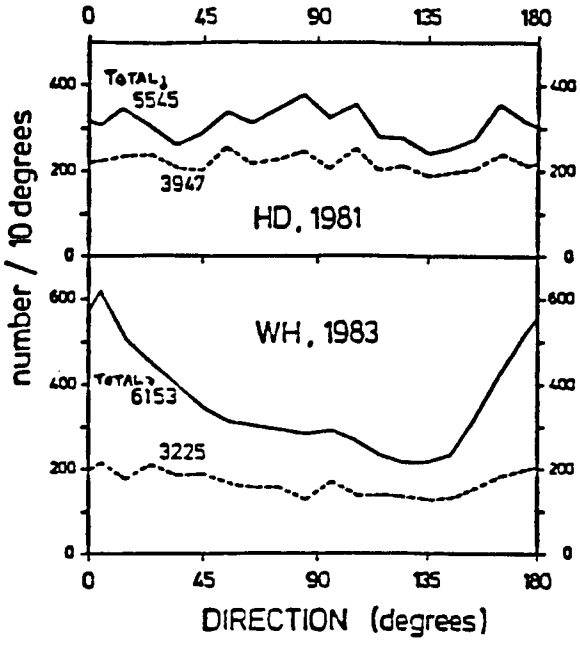

Figure 1. Histograms of ellipse tilt angle directions for long (HD) and short (WH) period wind perturbations at all heights (60–110 km): all data (solid line), and data below 80% confidence level (dashed line).

uniformly in direction. Also, the HD and WH data have different features; the former having peaks in N-S and E-W and the latter one peak at $\sim 10°$ E of N. Figures 2a and 2b show monthly % occurrence histograms for two years (these have been smoothed by a 1,1,1 filter before contouring). The HD data show that the E-W peak occurs mainly in the winter, whereas the N-S peak is present most of the year. The WH data show that N-S perturbations are more likely in the summer. Both types tend towards flatter distributions at the equinoxes.

Figures 3a and 3b divide the data into three height regions (the confidence limit had to be discarded in order to obtain sufficient data quantity).

3. MODELS

Five background wind filters are considered (Figure 4) by superposition of troposphere and stratosphere/lower mesosphere wind conditions. Except in model A, winds are assumed to vary from 0 to the maximum speed in each region. Model A assumes a minimum speed of 20 m/s (e.g., for tropospherically generated waves). Model A' (not shown) is the same as model A except that the minimum speed is 0 m/s. The hatched areas in this figure indicates forbidden phase velocities (the smallest circle excludes quasi-stationary waves in all models).

Three GW direction distributions are used: isotropic, predominantly E-W [$1 + \cos^4 (\phi - 90°)$], and northward biased [1 for $\phi = 90° - 270°$, and

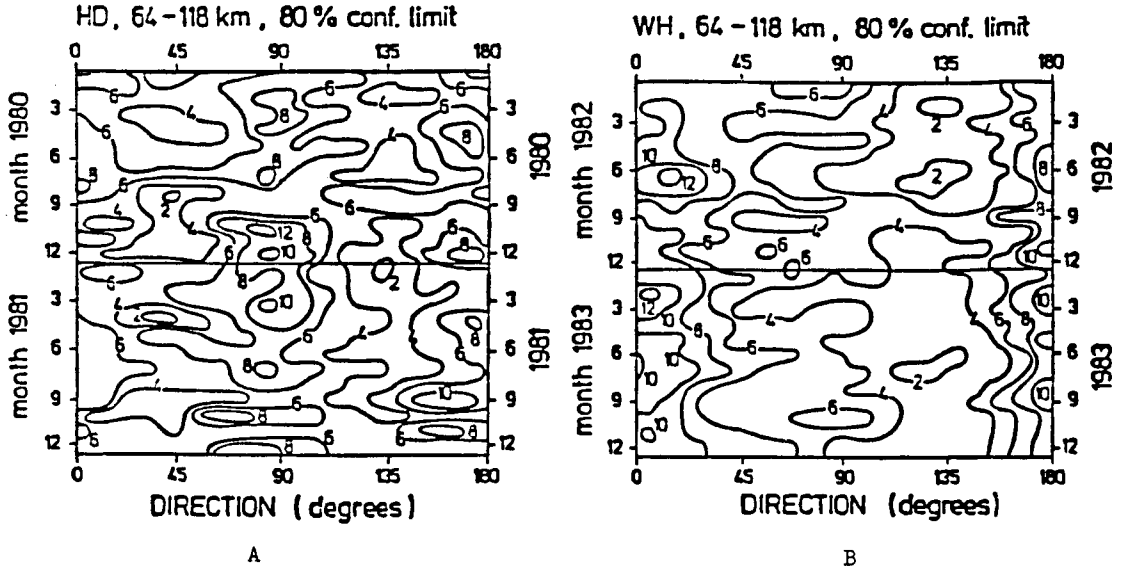

Figure 2. Smoothed monthly percentage (per 10° box) histograms over two years: long period (A) and short period (B). The nominal height range given corresponds to actual heights 60-110 km.

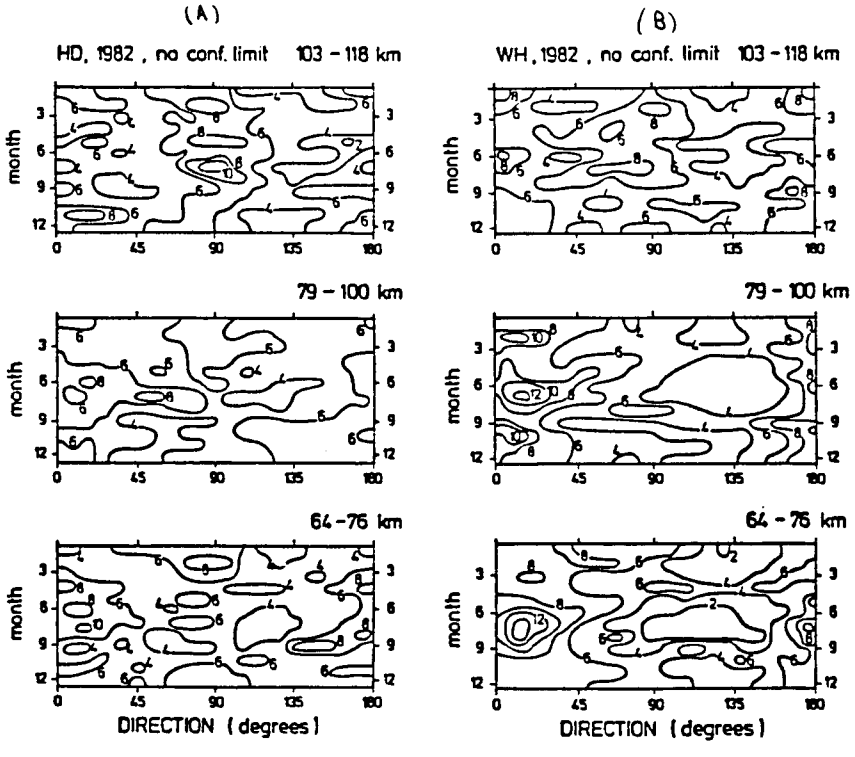

Figure 3. Height variation of direction distributions.

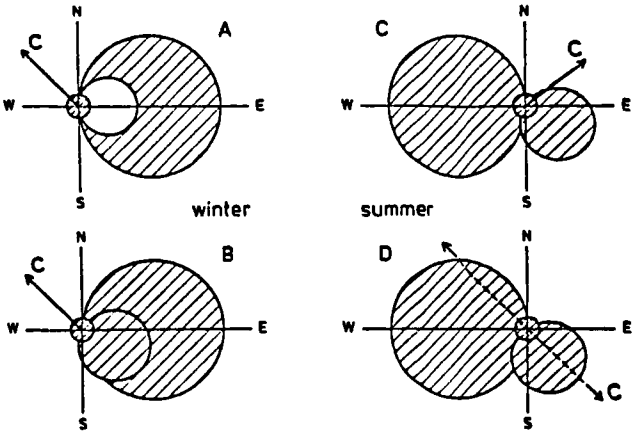

Figure 4. Model filters based on background seasonal wind characteristics. Maximum troposphere speed is 25 m/s; maximum stratosphere/lower mesosphere speed is 50 m/s; minimum wind speed (A only) is 20 m/s. Shaded areas indicate forbidden propagation for gravity waves.

1 + 0.3cos (ϕ) otherwise]. The last might simulate an increased northward flux created by thunderstorms and tornadoes in the summer. The phase speed distribution is Gaussian:

$$G(c) = \exp(c^2/2\sigma_c^2)$$

where σ_c is 30 m/s.

Predicted direction distributions created by combinations of filter and source assumptions are shown in Figure 5.

CONCLUSIONS

In such a short paper, it is impossible to discuss the results fully, but the following points may be made. For the WH data, it appears that filtering action by the predominant northwesterlies in the troposphere could be the cause of the bias towards NE perturbations in the mesosphere; also the fact that this bias is strongest in summer indicates an increase in N-S propagating waves, possibly due to thunderstorms or tornadoes. The HD data peak in the E-W direction is not easily explainable, unless the incident GW distribution has an E-W bias at these longer periods.

Wind Filter (see Fig. 4)	GW distrib. (N ↑, E →)	Curve
A'	⊙	1a
A	⊙	1b
A	⊙	2
B	⊙	3
C	⊙	4
C	⊙	5
D	⊙	6
C	⊙	7

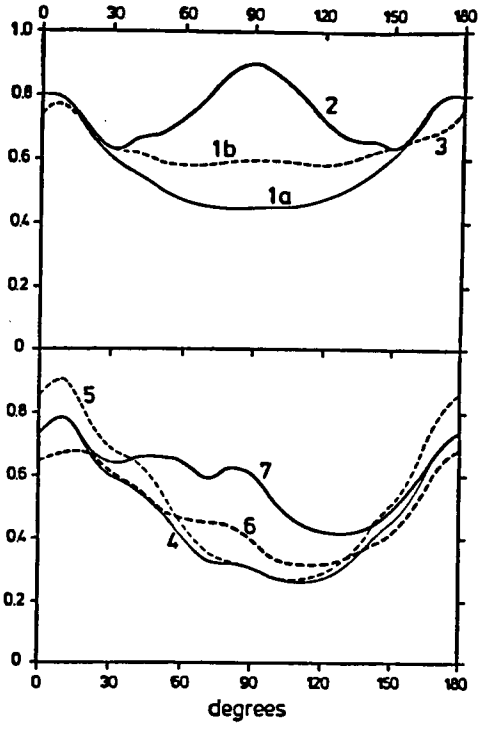

Figure 5. Theoretical direction distributions produced by combinations of different filter and GW direction distributions shown in the table (see text).